Helix-Coil Kinetics of Individual Polyadenylic Acid Molecules in a Protein Channel

Jianxun Lin,[1] Anatoly Kolomeisky,[2] and Amit Meller[1,*]

[1]*Department of Physics and Department of Biomedical Engineering, Boston University, Boston, Massachusetts 02215, USA*
[2]*Department of Chemistry, Rice University, Houston, Texas 77251, USA*

(Received 4 December 2009; published 15 April 2010)

Helix-coil transition kinetics of polyadenylic acid [poly(A)] inside a small protein channel is investigated for the first time, at the single molecule level. The confinement of a RNA molecule inside the channel slows its kinetics by nearly 3 orders of magnitude as compared to bulk measurements of free poly(A). These findings are related to the interaction energy of the RNA structure with the interior of the pore, explained by a simple two-state model. These results shed light on the way intermolecular interactions alter nucleic acid kinetics.

DOI: 10.1103/PhysRevLett.104.158101 PACS numbers: 87.15.H−, 87.15.kj

Under physiological conditions, polyadenylic acid [poly(A)] molecules form a secondary structure containing both helical and coiled domains, where the 20–50 base long helical portions are stabilized by stacking interactions of the adenine side groups [1–3]. The biological functions of poly(A) include interactions with various proteins [4,5], which are expected to significantly alter the kinetics of the poly(A) helix-coil transition as compared to that for free poly(A). Temperature-jump measurements at low-ionic (<0.1 M salt) conditions for free poly(A) have revealed first-order helix-coil kinetics with a sub-μs time scale [6]. Recent optical tweezers experiments using much longer poly(A) molecules have reported a plateau in the force-extension curve, indicating the presence of helix-coil domains [7].

To better understand the dynamical properties of poly(A) in the proximity of proteins, we have studied the spontaneous fluctuations of individual poly(A) strands threaded through a narrow protein channel (nanopore). Using an electric field, charged biopolymers can be drawn through a nanopore embedded in a lipid membrane separating two salt buffer-filled chambers. The presence of a molecule in the pore temporarily blocks and modulates the flow of ions, thus providing the means to directly probe individual biopolymers. Specifically, the bacterial toxin α-Hemolysin (α-HL) has been extensively used to probe nucleic acid structures [8–10], duplex formation and hairpin unzipping kinetics [11–14], and ssDNA/protein interactions [15,16]. Here, we probe the helix-coil transition kinetics of poly(A) molecules within the nanopore, and extract the corresponding enthalpic barriers. We find that the confinement of poly(A) inside the protein channel induces a remarkable slowing of the overall kinetics. This underlines the significant contribution of nucleic acid-protein interactions to the dynamics of biological systems.

Our experiment is shown schematically in Fig. 1(a). A solitary α-HL is incorporated into a freely suspended phospholipid bilayer as previously described [10], and the ion current flowing through the nanopore is measured under a voltage clamp. It is well known that when the *trans* chamber is positively biased, ssDNA or ssRNA from the *cis* chamber are electrophoretically threaded through the α-HL pore in a single-file manner [17]. Specifically, at 120 mV and room temperature, homopolymer poly(A) and

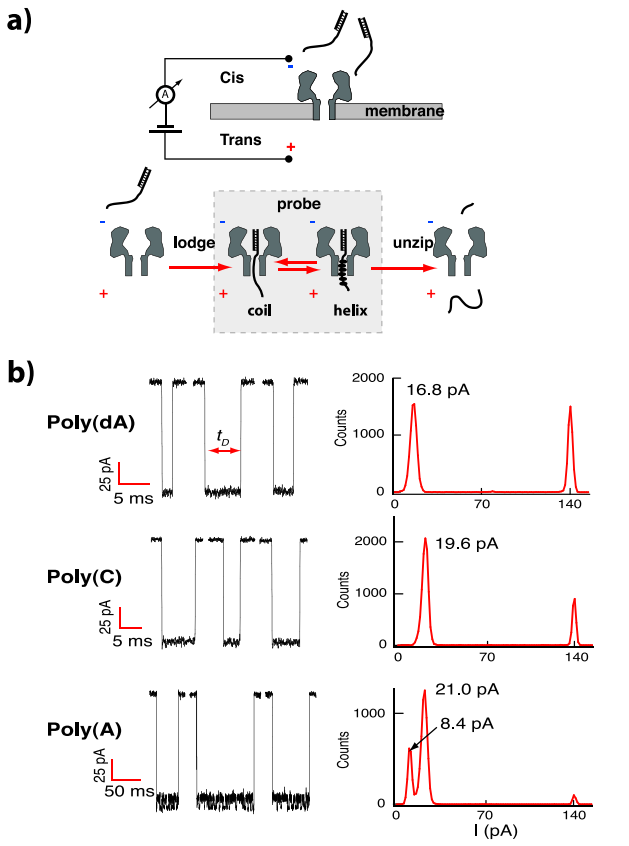

FIG. 1 (color online). (a) A schematic illustration of the nanopore experiment. (b) The left-hand panel shows representative events for duplex dA_{50}, duplex C_{25}, and duplex A_{25}, from top to bottom; the right-hand panel displays the corresponding all-point current histograms.

polydeoxyadenylic acid [poly(dA)] translocate across an α-HL channel with an average time of 12 μs/nt and 3 μs/nt, respectively [9,18,19]. The fourfold difference between these translocation time scales has been associated with the larger cross-sectional area (~2.1 nm) of the helical structure of poly(A) as compared to poly(dA) [9]. The poly(A) helix must be denatured when it is threaded through the narrowest constriction of the α-HL (~1.4 nm), causing a retardation in the translocation process. Since the β-barrel of α-HL (past the narrowest constriction) is on average 2.2 nm [20], the helical poly(A) can in principle be formed in the channel. However, this coil to helix transformation has not been observed to date, presumably due to the short residence time of poly(A) inside the α-HL.

To observe poly(A) kinetics, we rely upon the fact that duplex nucleic acids (~2.2 nm) cannot be threaded through the α-HL's smallest constriction [13]. Therefore, when duplex nucleic acids with a single-stranded overhang are in the *cis* chamber, the single-stranded portion may be threaded through the pore, but the molecule remains effectively arrested for an extended period of time until the trailing duplex region is completely unzipped [Fig. 1(a), lower panel] [14]. The left panel of Fig. 1(b) displays representative events collected at 25 °C and 120 mV for three molecules: (i) *duplex* dA_{50}, a DNA duplex with a 50-base poly(dA) overhang, (ii) *duplex* C_{25}, a RNA duplex with a 25-base poly(C) overhang, and (iii) *duplex* A_{25}, a RNA duplex with a 25-base poly(A) overhang. The duplex region in all molecules has the same 10-bp sequence. We note two salient features differentiating *duplex* A_{25} from *duplex* C_{25} and *duplex* dA_{50}. First, the dwell time (t_D) of *duplex* A_{25} is nearly an order of magnitude longer than that of *duplex* C_{25}. Second, the ion current signal associated with *duplex* A_{25} displays large fluctuations.

We further characterize these ion current fluctuations using the all-point histograms shown in the right-hand panel of Fig. 1(b). Focusing first on the bottom-most histogram for the poly(A) sample, we observe two distinct blocked current levels at 21 and 8.2 pA. In contrast, the poly(C) and poly(dA) sample each produce a single blocked current level at 19.2 and 16.4 pA, respectively. We note that the higher current state of poly(A) is similar to that of poly(dA). The second, noticeably lower current state of poly(A) is indicative of a more compact structure with a larger cross section inside the pore. The absence of a similar current state for the poly(dA) molecule, which differs from poly(A) only through lack of a 2′-hydroxyl group, is also in line with the hypothesis that the low current state is related to the stronger propensity of poly(A) to form a helix [6]. In the inset of Fig. 2, we overlaid a helical poly(A) to scale with the well-known structure of α-HL [20]. The poly(A) is drawn as a ninefold A-form helix, based on the crystal structure of poly(A) trimmers [3]. It is evident that the poly(A) helix fits inside the β barrel of the channel.

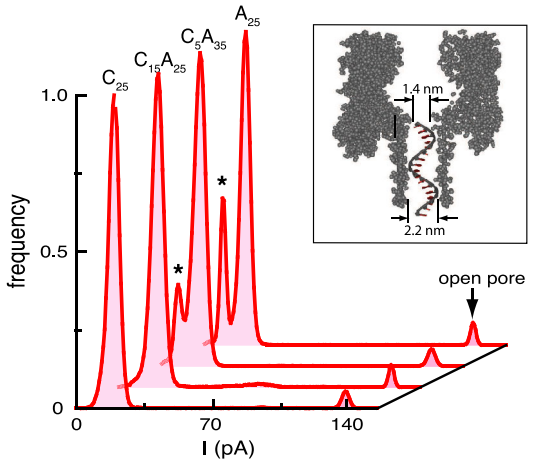

FIG. 2 (color online). All-point current histograms of 4 RNA molecules as indicated by a single-stranded overhang. The inset is a schematic cross-sectional view of the poly(A) helix inside the β barrel of α-HL, to scale.

Furthermore, since the poly(C) molecules produce only a single blocked current state, we hypothesize that inserting short poly(C) "spacers" between the duplex region and the poly(A) tail would allow us to map out the range in which ion current fluctuations due to structural change of poly(A) are observed. Given that the β-barrel channel is ~5 nm long, we theorize that a transition from two blockage levels to only one would occur when this spacing is ~12 bases [7]. To test this idea, we create two additional RNA molecules with the same 10-bp duplex part as before: (1) A *duplex* C_5A_{35} and (2) a *duplex* $C_{15}A_{25}$. As shown in Fig. 2, *duplex* C_5A_{35} clearly displays two blocked current levels, while *duplex* $C_{15}A_{25}$ produces blockade signals that are indistinguishable from those of *duplex*-C_{25}. We therefore conclude that the two-state fluctuations are indeed caused by the secondary structure of polyadenine bases inside the β-barrel, and that the length of this region is up to 15 bases.

A time-resolved analysis of individual poly(A) molecules undergoing two-state fluctuations is given in Fig. 3. A single current threshold [dashed line in Fig. 3(a)] is defined to automatically fragment each event into the high and low transition times, t_{high} and t_{low}, respectively. Analyzing >2000 transitions, we find that both distributions can be fitted using monoexponentials, which yield the characteristic lifetimes of the helix and the coil state, τ_{helix} and τ_{coil}, respectively. The millisecond time scale here is nearly 3 orders of magnitude longer than that observed for free poly(A) in bulk [6]. We perform a similar analysis for 15 additional experiments at different temperatures and voltages. Figure 4 shows an Arrhenius plot of these data fitted with the equation $\tau = \tau_0 \exp(\Delta H^{\ddagger}_{\text{pore}}/k_B T)$, allowing us to extract the respective enthalpic barriers for coil to helix ($\Delta H^{\ddagger}_{CH,\text{pore}}$) and helix to coil transitions ($\Delta H^{\ddagger}_{HC,\text{pore}}$). Our results are summarized in Fig. 4 inset. We note that while $\Delta H^{\ddagger}_{CH,\text{pore}}$ is insensitive to the applied voltage

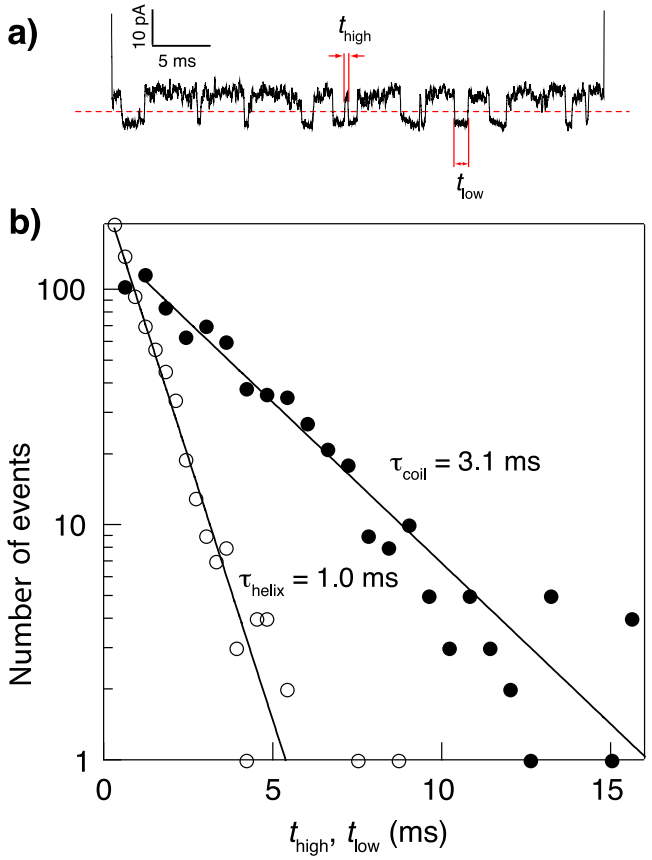

FIG. 3 (color online). (a) Time-resolved analysis of two-state fluctuations for poly(A) samples using a single current threshold (dashed line) to extract t_{high} and t_{low}. (b) Distribution of t_{high} and t_{low} (○) at 120 mV and 25 °C. Both distributions are fitted with monoexponentials, which provide τ_{coil} and τ_{helix}, respectively.

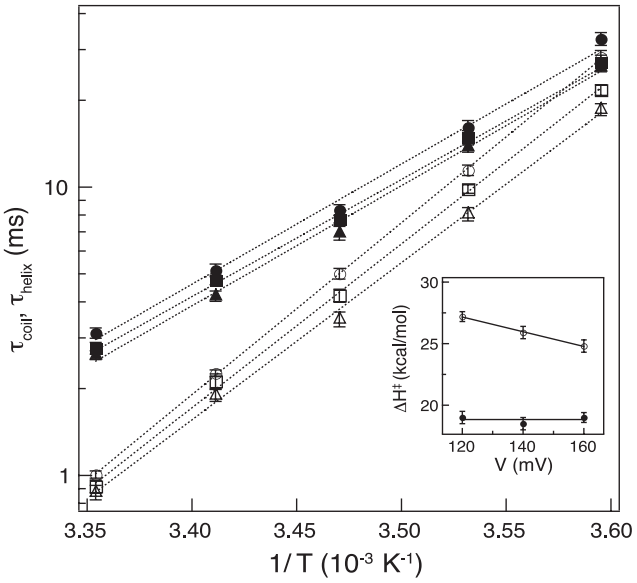

FIG. 4. τ_{coil} (solid symbol) and τ_{helix} (open symbol) as a function of temperature at 3 voltages: 120 mV (●, ○), 140 mV (■, □), and 160 mV (▲, △). The Arrhenius fits (dashed lines) give the enthalpic barriers $\Delta H^{\ddagger}_{pore}$. The inset shows the change in $\Delta H^{\ddagger}_{pore}$ for coil (•) and helix (○) as a function of voltage with linear fits.

(~19 kcal/mol), $\Delta H^{\ddagger}_{HC,pore}$ decreases from 27.2 kcal/mol at 120 mV to 24.8 kcal/mol at 160 mV.

The bulk kinetics of poly(A) helix-coil transition are described using a two-state model in Fig. 5(a) [6]. We adopt a similar two-state model for our nanopore system. However, we consider two additional effects: (i) the tilt of the energy landscape induced by the applied voltage, and (ii) the confinement of the nucleic acids in the pore. The magnitudes of both enthalpic barriers in the nanopore system are substantially larger than their corresponding bulk values ($\Delta H^{\ddagger}_{CH,bulk} = 4$ kcal/mol and $\Delta H^{\ddagger}_{HC,bulk} =$ 15 kcal/mol) [6], thus the free energy surface in the absence of applied voltage can be drawn as the dashed line in Fig. 5(b). In the presence of voltage, the two energy levels are in principle biased. However, given our results showing that $\Delta H^{\ddagger}_{CH,pore}$ is insensitive to voltage variation, as a first approximation we can neglect the shift in the level of the coil state. The resulting energy landscape is displayed as a solid red line in Fig. 5(b). We define the free energy change for moving the coil or the helix from the bulk into the pore as ΔG_C or ΔG_H. Specifically, we can write $\Delta G_C = N_C\varepsilon_C - T\Delta S_C$, where the first term reflects the coil-pore interaction energy of N_C coiled monomers, each possessing an energy ε_C (negative for attraction or positive for repulsion), and the second term reflects the entropic contribution. A similar argument for the helical state yields $\Delta G_H = N_H\varepsilon_H - T\Delta S_H + \frac{1}{2}(q_H N_H - q_C N_C)V$, where the additional term represents the electrostatic contribution due to moving $N_H - N_C$ monomers back towards the pore against the external field of strength V; q_H, and q_C represent the effective charge per monomer for the helix and coil states, respectively.

At thermal equilibrium, we can relate the lifetime of finding a biopolymer coil inside the pore or in the bulk by the Boltzmann factor $e^{-\Delta G_C/k_BT}$. Accounting for the Arrhenius kinetics in both pore and bulk, namely, $\tau_C \sim e^{\Delta H^{\ddagger}_{CH}/k_BT}$, it can be shown that for the coil to helix transition $\Delta H^{\ddagger}_{CH,pore} - \Delta H^{\ddagger}_{CH,bulk} = -N_C\varepsilon_C$. Following similar arguments, for the helix to coil transition, $\Delta H^{\ddagger}_{HC,pore} - \Delta H^{\ddagger}_{HC,bulk} = -N_H\varepsilon_H - \frac{1}{2}(q_H N_H - q_C N_C)V$. The linear dependence of $\Delta H^{\ddagger}_{HC,pore}$ on voltage is in agreement with our data (inset of Fig. 4), which yield $\frac{1}{2}(q_H N_H - q_C N_C) \cong 0.06$ kcal/(mol · mV). By using $q_C \cong 0.14e$ [14], and a steric estimation of $N_H \cong 16$, $N_C \cong 8$ [3,21], we can estimate $q_H \cong 0.4e$. The larger value of q_H is consistent with the more compact structure of the helix, which would in turn exclude more counterions from the channel, decreasing screening and increasing the effective charge. Our model can be also used to estimate the interaction energies, which are $\varepsilon_C = -1.9$ kcal/mol and $\varepsilon_H = -1.2$ kcal/mol. Therefore, both interactions are

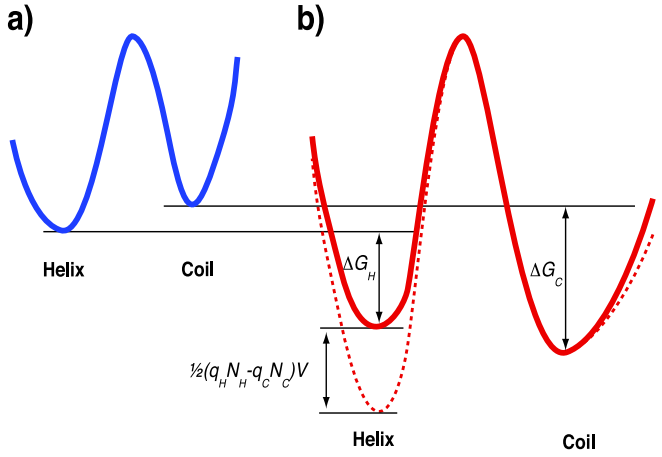

FIG. 5 (color online). (a) Sketch of the free energy landscape of poly(A) helix-coil transition in bulk. (b) Sketch of the modified free energy landscape of the poly(A) helix-coil transition in the pore. The dashed line represents the landscape with no applied voltage, while the solid line reflects the tilting effect of voltage.

attractive, creating slower confined kinetics for both states than those observed in bulk. But as expected, the attraction to the pore per monomer is smaller in the helix than for the coil, probably due to stronger steric interactions.

Returning to Fig. 1, we postulate that the dwell time of duplex poly(A) is governed by two independent processes, unzipping and unstacking. In order to translocate to the *trans* side, not only the duplex region needs to be unzipped, but also the poly(A) strand has to be unstacked into coil structure. This hypothesis is supported by the following two observations. (i) We find that >90% of the last transition state before translocation is the coiled state [see Fig. 3(a)]. (ii) The time scale of helix-coil transition is comparable to the unzipping time, thus the unzipped duplex part has high enough probability to reanneal before successful translocation.

In conclusion, by arresting single poly(A) molecules inside a nanopore, we are able to directly observe and characterize discrete two-state kinetics, which is associated with a helix-coil transition. Our measurements reveal, however, that the helix-coil transition kinetics of the pore-confined poly(A) molecules are slowed by nearly 3 orders of magnitude as compared to the kinetics of free poly(A) in bulk. We attribute this to the stabilizing effect of confining the RNA inside a ~2.2 nm protein channel. Despite the simplistic nature of our two-state model, it allows us to extract useful physical parameters. The biological function of poly(A) entails strong interactions with proteins, specifically, the cocrystal structure of Poly(A) Binding Proteins (PABP) and 11-base poly(A) shows that upon binding, poly(A) adopts an extended conformation in the molecular trough, which is of similar dimensions to our system [22]. The α-HL channel, while different in structure from PABP, allows us to explore the poly(A) kinetics in close proximity to a protein surface, providing insight on the stabilizing effects of the protein-poly(A) interactions.

A. M. acknowledges support from HFSP grant RGP0036-2005. A. K. acknowledges support from NSF grant ECCS-0708765, and the Welch Foundation (grant C-1554).

*ameller@bu.edu

[1] D. N. Holcomb and I. Tinoco, Jr., Biopolymers **3**, 121 (1965).
[2] M. Leng and G. Felsenfeld, J. Mol. Biol. **15**, 455 (1966).
[3] W. Saenger, J. Riecke, and D. Suck, J. Mol. Biol. **93**, 529 (1975).
[4] Y. V. Svitkin, EMBO J. **28**, 58 (2009).
[5] D. A. Mangus, M. C. Evans, and A. Jacobson, Genome Biol. **4**, 223 (2003).
[6] T. G. Dewey and D. H. Truner, Biochemistry **18**, 5757 (1979).
[7] Y. Seol *et al.*, Phys. Rev. Lett. **98**, 158103 (2007).
[8] J. Kasianowicz *et al.*, Proc. Natl. Acad. Sci. U.S.A. **93**, 13 770 (1996).
[9] M. Akeson *et al.*, Biophys. J. **77**, 3227 (1999).
[10] A. Meller *et al.*, Proc. Natl. Acad. Sci. U.S.A. **97**, 1079 (2000).
[11] W. Vercoutere *et al.*, Nat. Biotechnol. **19**, 248 (2001).
[12] S. Howorka *et al.*, Proc. Natl. Acad. Sci. U.S.A. **98**, 12 996 (2001).
[13] A. F. Sauer-Budge *et al.*, Phys. Rev. Lett. **90**, 238101 (2003).
[14] J. Mathé *et al.*, Biophys. J. **87**, 3205 (2004).
[15] C. P. Goodrich *et al.*, J. Phys. Chem. B **111**, 3332 (2007).
[16] B. Hornblower *et al.*, Nat. Methods **4**, 315 (2007).
[17] A. Meller, L. Nivon, and D. Branton, Phys. Rev. Lett. **86**, 3435 (2001).
[18] T. Z. Butler, J. H. Gundlach, and M. A. Troll, Biophys. J. **90**, 190 (2006).
[19] J. Mathé *et al.*, Proc. Natl. Acad. Sci. U.S.A. **102**, 12 377 (2005).
[20] L. Song *et al.*, Science **274**, 1859 (1996).
[21] J. B. Mills, E. Vacano, and P. J. Hagerman, J. Mol. Biol. **285**, 245 (1999).
[22] R. C. Deo *et al.*, Cell **98**, 835 (1999).